PHASE QUALITY OPTIMIZATION TECHNIQUES AND LIMITATIONS IN POLARIMETRIC DIFFERENTIAL SAR INTERFEROMETRY

Rubén Iglesias, **Dani Monells**, Xavier Fabregas,Jordi J.Mallorqui, Albert Aguasca, *and* Carlos López-Martínez

Remote Sensing Lab. (RSLab), Universitat Politècnica de Catalunya (UPC)
D3 - Campus Nord, UPC, 08034, Barcelona, Spain
E-mail: ruben.iglesias@tsc.upc.edu, dmonells@tsc.upc.edu

Outline

- Introduction
- DInSAR Pixel Selection
- Polarimetric Scattering Matrix and Basis Transformation
- Vector Interferometry
- Coherence Optimization techniques
- Amplitude Dispersion Optimization techniques
- Test-Sites
- Optimization Techniques Comparison
  - ➔ Coherence
  - ➔ Amplitude Dispersion
- Fully-Polarimetric DInSAR processing
- DInSAR results

Introduction

- **DInSAR** techniques have been limited to the **single polarization** case

- Launch of several **satellites** with **polarimetric capabilities**
  - ➔ Envisat: Dual-Pol, C-Band, launched at 2002.
  - ➔ ALOS: Quad-Pol, L-Band, launced at 2006.
  - ➔ TerraSAR-X: Dual-Pol, X-Band, launched at 2007.
  - ➔ Radarsat-2: Quad-Pol, C-Band, launched at 2007.
  - ➔ Cosmo-Skymed: Dual-Pol, X-Band, launched at 2007.
  - ➔ Tandem-X: Quad-Pol, X-Band, launched at 2010.
  - ➔ **Future missions**
    - Sentinel: Dual-Pol, C-band, programed for 2013
    - ALOS-2: Quad-Pol, L-Band, programed for 2013
    - Radarsat Constellation: Quad-Pol, C-band, programed for 2014-2015

Objective

Enhance the phase quality of the interferograms to be processed by the DInSAR algorithms with the proper combination of the available polarimetric channels

- **Fully polarimetric UPC's Ground-Based SAR (RISKSAR)**

DInSAR Pixel Selection

- Due to **decorrelation** → Information cannot be extracted from all the pixels → **Pixel selection** is mandatory
- **Two different criteria** are mainly employed for the estimation of the pixels quality:

→ **The coherence stability**

$$\gamma = \frac{E[P_1 \cdot P_2^*]}{\sqrt{E\left[|P_1|^2\right] \cdot E\left[|P_2|^2\right]}} \qquad |\gamma| = \frac{SNR}{SNR+1} \qquad 0 \le |\gamma| \le 1$$

- No theoretical minimum of acquisitions

-Spatial resolution loss

→ **Amplitude dispersion**

$$\sigma_v \approx \frac{\sigma_n}{g} \approx \frac{\sigma_A}{m_A} \equiv D_A$$

- Full resolution method

- Minimum of 20-30 images required

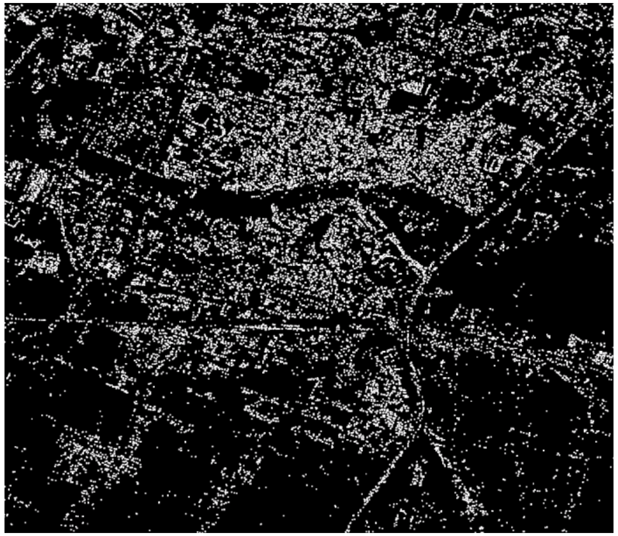

Coherence pixel selection
Coh>0.6 ML=5x5

TerraSAR-X SLC of Murcia (Spain)

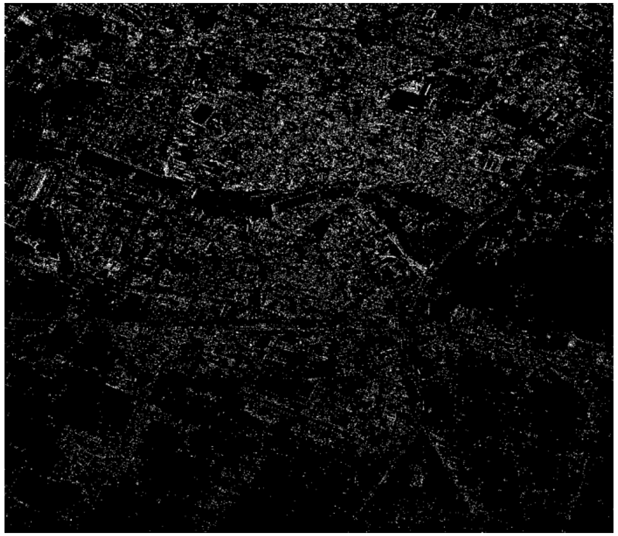

Amplitude Dispersion pixel selection
DA<0.25

Polarimetric Scattering Matrix and Basis Transformation

- **Scattering matrix**

$$\mathbf{S}_{hv} = \begin{bmatrix} S_{hh} & S_{hv} \\ S_{hv} & S_{vv} \end{bmatrix}$$

- **Polarimetric Basis Transformation**

$$\mathbf{S}_{xy} = \begin{bmatrix} S_{xx} & S_{xy} \\ S_{xy} & S_{yy} \end{bmatrix} = \mathbf{U}_2{}^T \mathbf{S}_{hv} \mathbf{U}_2$$

$$\mathbf{U}_2 = \begin{bmatrix} \cos\psi & -\sin\psi \\ \sin\psi & \cos\psi \end{bmatrix} \begin{bmatrix} \cos\chi & j\sin\chi \\ j\sin\chi & \cos\chi \end{bmatrix} \begin{bmatrix} e^{+j\phi_0} & 0 \\ 0 & e^{-j\phi_0} \end{bmatrix}$$

- **Interferometric coherence**

$$\boxed{\gamma_{xy} = \left|\gamma_{xy}\right| e^{j\phi_{xy}} = \frac{\sum_{i=1}^{N_L} S_{xy,1} S_{xy,2}^*}{\sqrt{\sum_{i=1}^{N_L} \left|S_{xy,1}\right|^2 \sum_{i=1}^{N_L} \left|S_{xy,2}\right|^2}}}$$

Vector Interferometry

- **Pauli** $$\mathbf{k}_i = \frac{1}{\sqrt{2}}\left[S_{hh,i}+S_{vv,i}, S_{hh,i}-S_{vv,i}, 2S_{hv,i}\right]^T$$
- **PolInSAR vector** $$\mathbf{k} = \left[\mathbf{k}_1^T, \mathbf{k}_2^T\right]^T.$$
- **T6** $$\mathbf{T}_6 = E\left\{\mathbf{k}\mathbf{k}^H\right\} = \begin{bmatrix} \mathbf{T}_{11} & \mathbf{\Omega}_{12} \\ \mathbf{\Omega}_{12}^H & \mathbf{T}_{22} \end{bmatrix}$$
- **Projection vector** $$S_i = \mathbf{w}_i^H \mathbf{k}_i$$
- **Generalized Coherence**

$$\gamma(\mathbf{w}_1,\mathbf{w}_2) = \frac{\mathbf{w}_1^H \mathbf{\Omega}_{12}\mathbf{w}_2}{\sqrt{\mathbf{w}_1^H \mathbf{T}_{11}\mathbf{w}_1 \mathbf{w}_2^H \mathbf{T}_{22}\mathbf{w}_2}}$$

Avoid changes in the phase center

$$\xrightarrow[\mathbf{w}_1=\mathbf{w}_2]{}$$

$$\gamma(\mathbf{w}) = \frac{\mathbf{w}^H \mathbf{\Omega}_{12}\mathbf{w}}{\sqrt{\mathbf{w}^H \mathbf{T}_{11}\mathbf{w}\ \mathbf{w}^H \mathbf{T}_{22}\mathbf{w}}}$$

Coherence Optimization techniques

- **Best**

  → Selecting the polarimetric channel providing the highest coherence for each interferogram ⇔ Select the channel that is less affected by decorrelation factors for each pair of images

  $$|\gamma_{Best}| = \max\{|\gamma_{hh}|, |\gamma_{hv}|, |\gamma_{vv}|\}$$

- **Double Scattering Mechanism (DSM)** $\mathbf{w}_1 \neq \mathbf{w}_2$: Consider different phase centers → **Not Suitable for DInSAR**

  → Finding the projection vector **w** that optimizes the generalized coherence $\gamma(\mathbf{w}_1, \mathbf{w}_2) = \frac{\mathbf{w}_1^H \mathbf{\Omega}_{12} \mathbf{w}_2}{\sqrt{\mathbf{w}_1^H \mathbf{T}_{11} \mathbf{w}_1 \mathbf{w}_2^H \mathbf{T}_{22} \mathbf{w}_2}}$

  Cloude, S.R.; Papathanassiou, K.P.; "Polarimetric SAR interferometry," *IEEE Transactions on Geoscience and Remote Sensing*,, Sep 1998

- **Equal Scattering Mechanism (ESM)** $\mathbf{w}_1 = \mathbf{w}_2$: Consider same phase centers → **Suitable for DInSAR**

  → Finding the projection vector **w** that optimizes the generalized coherence $\gamma(\mathbf{w}) = \frac{\mathbf{w}^H \mathbf{\Omega}_{12} \mathbf{w}}{\sqrt{\mathbf{w}^H \mathbf{T}_{11} \mathbf{w} \; \mathbf{w}^H \mathbf{T}_{22} \mathbf{w}}}$

  - Parameterization of the projection vector w

$$\mathbf{w} = \begin{bmatrix} \cos\alpha \\ \sin\alpha\cos\beta e^{j\delta} \\ \sin\alpha\sin\beta e^{j\gamma} \end{bmatrix} \Rightarrow \mathbf{w}_{opt} \Rightarrow \phi_{ESM} = angle\left\{\left(\mathbf{w}_{opt,ESM}^H \mathbf{k}_i\right)\left(\mathbf{w}_{opt,ESM}^H \mathbf{k}_j\right)^*\right\}$$

Disadvantages
High Computational Cost

Coherence Optimization techniques

• **Numerical Iterative solution**

Colin, E.; Titin-Schnaider, C.; Tabbara, W.; , "An interferometric coherence optimization method in radar polarimetry for high-resolution imagery," *IEEE Transactions on Geoscience and Remote Sensing, Jan. 2006*

→ Assumes $T_{11} \approx T_{22}$

$$\mathbf{T} = \frac{\mathbf{T}_{11} + \mathbf{T}_{22}}{2} \Rightarrow \hat{\gamma}(\mathbf{w}) = \frac{\mathbf{w}^H \mathbf{\Omega}_{12} \mathbf{w}}{\mathbf{w}^H \mathbf{T}\,\mathbf{w}} \quad |\hat{\gamma}| \leq |\gamma| \Rightarrow$$

Solution based on calculating the numerical radius of

$$T^{-1/2}\mathbf{\Omega}_{12}T^{-1/2}$$

→ Optimized interferogram $\phi_{ESM} = angle\left\{\left(\mathbf{w}_{opt,ESM}^H \mathbf{k}_i\right)\left(\mathbf{w}_{opt,ESM}^H \mathbf{k}_j\right)^*\right\}$

→ **Advantages** → Low computational cost

→ **Disadvantages** → Needs polarimetric stability to reach the optimum of coherence

Wishart distance

$$\mathrm{d} = \mathrm{tr}\left(\mathrm{T}_{11}^{-1} \cdot \mathrm{T}_{22}\right) + \mathrm{tr}\left(\mathrm{T}_{11}^{-1} \cdot \mathrm{T}_{22}\right) - 6 \Rightarrow$$

When polarimetric stability does not apply the optimized differential phase may be affected

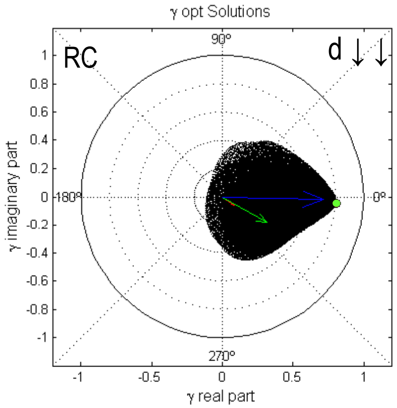

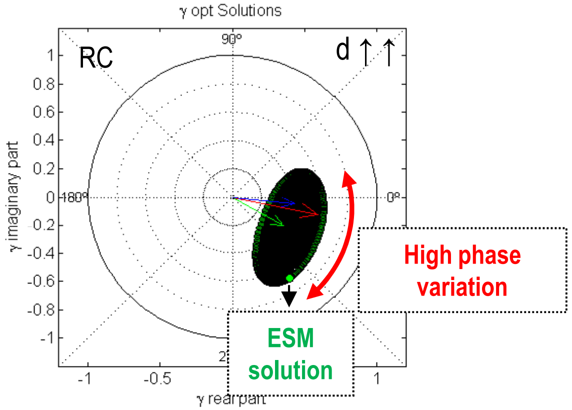

Coherence Optimization techniques

- **Suboptimum mecahnism (SOM)**

Explore all the (ψ,χ) space in order to find the polarization basis transform providing the highest coherence value among all the co-polar γ_{aa} and cross-polar γ_{ab} coherence values

$$\left|\gamma_{SOM}\right| = \max_{(\psi,\chi)}\left\{\left|\gamma_{aa}(\psi,\chi)\right|,\left|\gamma_{ab}(\psi,\chi)\right|\right\}$$

$$\gamma_{aa} = \frac{E\left\{S_{aa,1}S_{aa,2}\right\}}{\sqrt{E\left\{\left|S_{aa,1}\right|^2\right\}E\left\{\left|S_{aa,2}\right|^2\right\}}}$$

$$\gamma_{ab} = \frac{E\left\{S_{ab,1}S_{ab,2}\right\}}{\sqrt{E\left\{\left|S_{ab,1}\right|^2\right\}E\left\{\left|S_{ab,2}\right|^2\right\}}}$$

Disadvantages

High Computational cost

Co-polar coherence γ_{aa} values as a function of (ψ,χ) for four representative pixels, with different values of $|\gamma_{Best}|$

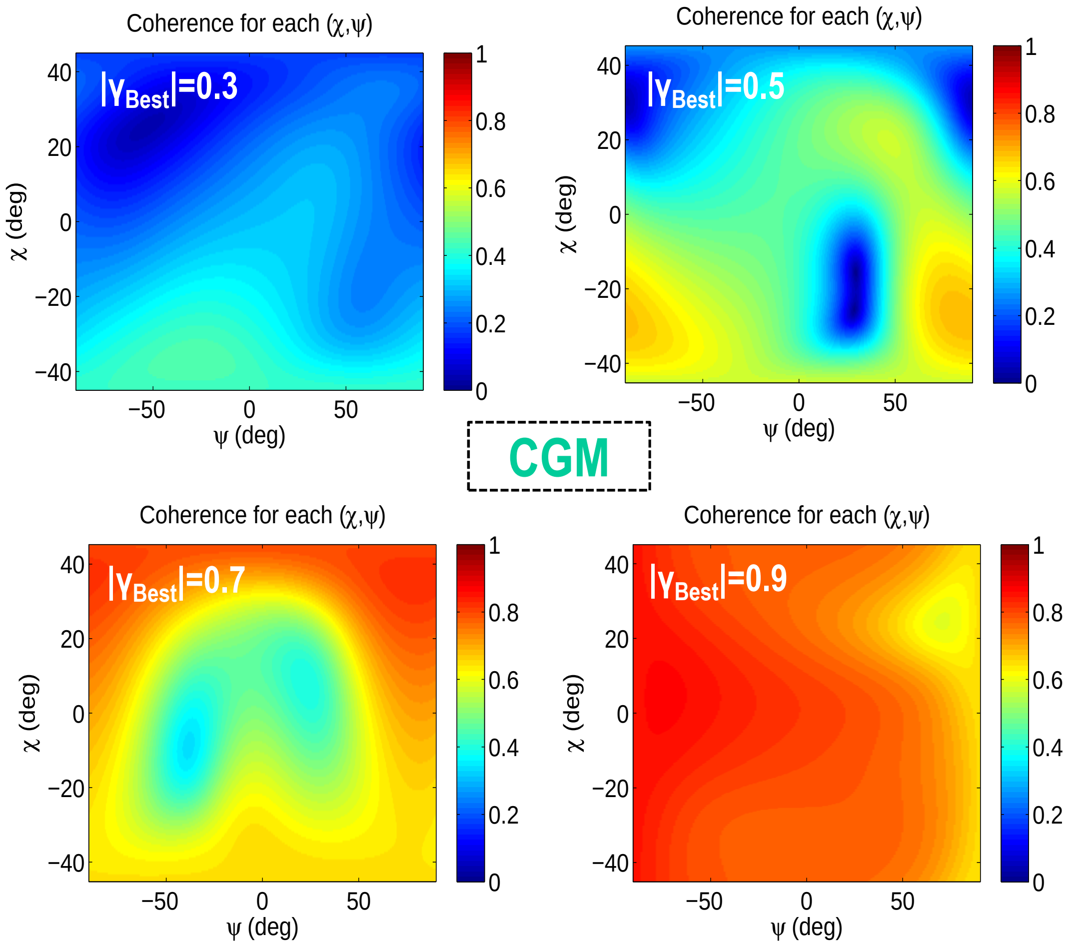

Amplitude Dispersion Optimization techniques

- **Best**

Selecting the polarimetric channel providing the highest coherence for each interferogram

$$D_{A,Best} = \min\left\{D_{A,hh}, D_{A,hv}, D_{A,vv}\right\}$$

- **ESM**

Finding the projection vector **w** that optimizes the generalized D_A

$$D_A(\mathbf{w}) = \frac{1}{\left\langle\left|\mathbf{w}^H \cdot \mathbf{k}\right|\right\rangle} \cdot \sqrt{\frac{1}{N}\sum_{i=1}^{N}\left(\left|\mathbf{w}^H . \mathbf{k}_i\right| - \left\langle\left|\mathbf{w}^H \cdot \mathbf{k}\right|\right\rangle\right)^2}$$

$$\left\langle\left|\mathbf{w}^H \cdot \mathbf{k}\right|\right\rangle = \frac{1}{N} \cdot \sum_{i=1}^{N}\left|\mathbf{w}^H \cdot \mathbf{k}_i\right|$$

- **SOM**

Explore all the *(ψ,χ)* space in order to find the polarization basis transform providing the minimum D_A value among all the co-polar DA_{aa} and cross-polar DA_{ab} amplitude Dispersion values

$$D_{A,SOM} = \min_{(\psi,\chi)}\left\{D_{A,aa}(\psi,\chi), D_{A,ab}(\psi,\chi)\right\}$$

Fully-polarimetric Ground Based-SAR data-set (Canillo)

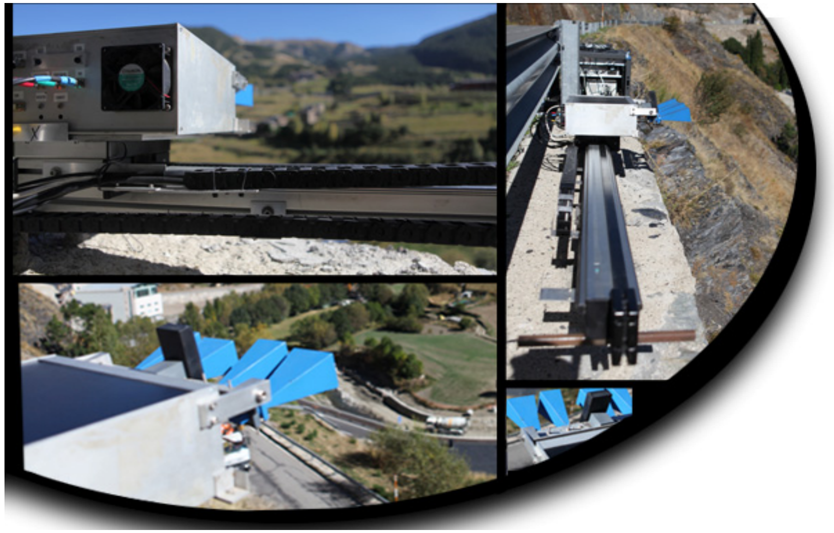

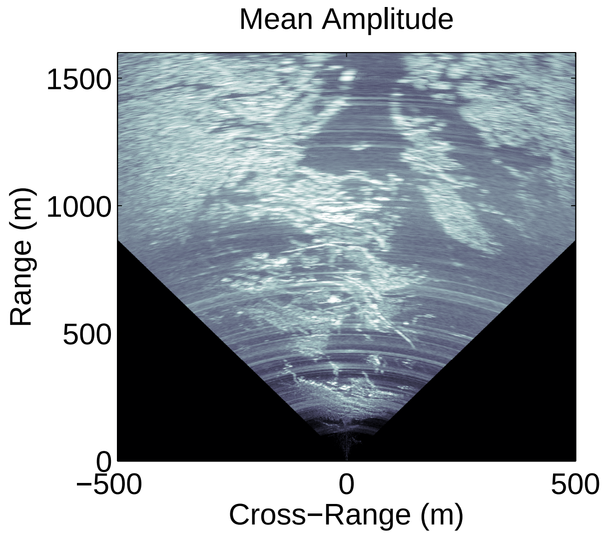

→ **Dataset: 10 Full-Pol Acquisitions**

→ **Temporal span: From October 2010 to October 2011**

→ **Objective: Landslide monitoring**

→ **Canillo Processing parameters**

- **X-Band** 9.65 GHz
- **Full Polarization** Mode: VV VH HV HH
- Maxim Range Distance: **1.6 km**
- Range resolution: **1.25 m**
- Cross-Range Resolution **@ 800m (L=2m): 3 m**

Fully-polarimetric Radarsat-2 data-set (Barcelona)

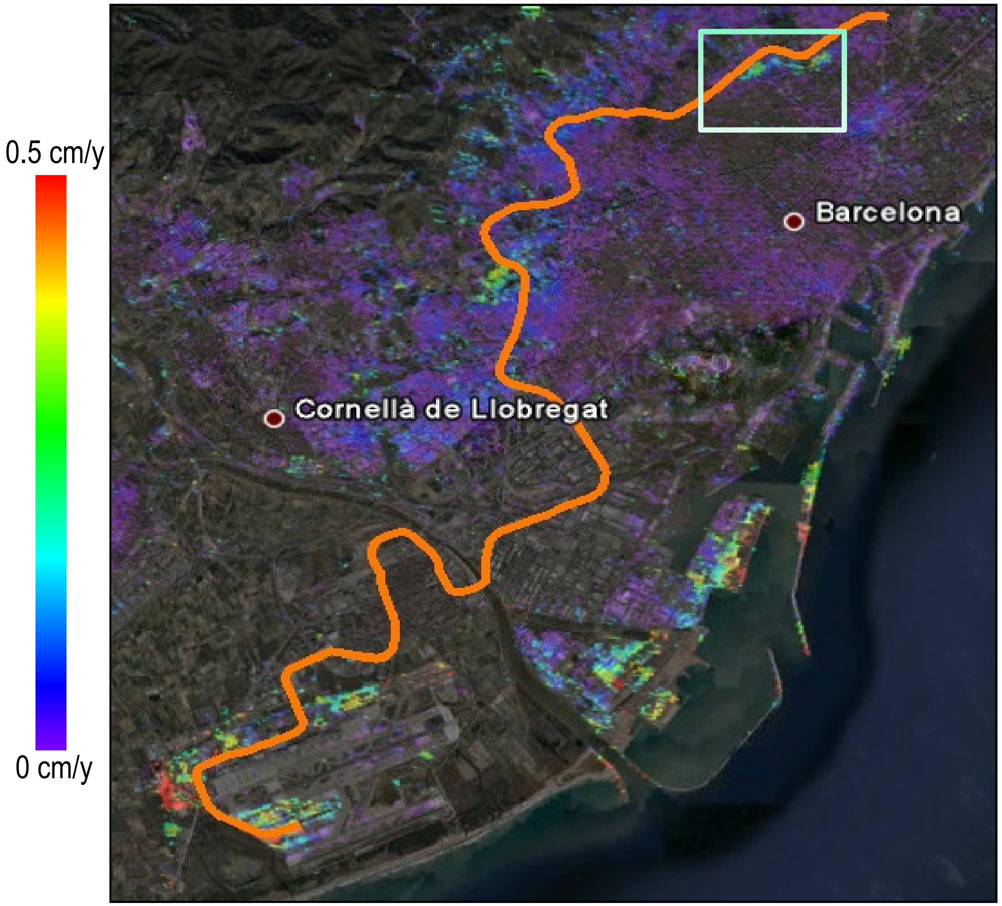

- Location: Barcelona
- Sensor: Radarsat-2
- Band: C
- Dataset: 37 Fine Quad-Pol Acquisitions
- Temporal span: From January 2010 to July 2012
- Diagnosis: Subsidence due to underground construction

Coherence Optimization Techniques Comparison

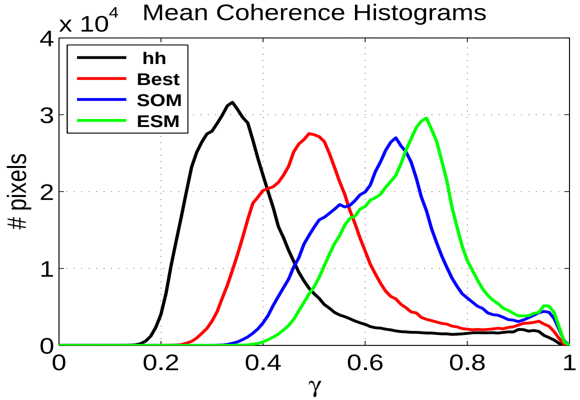

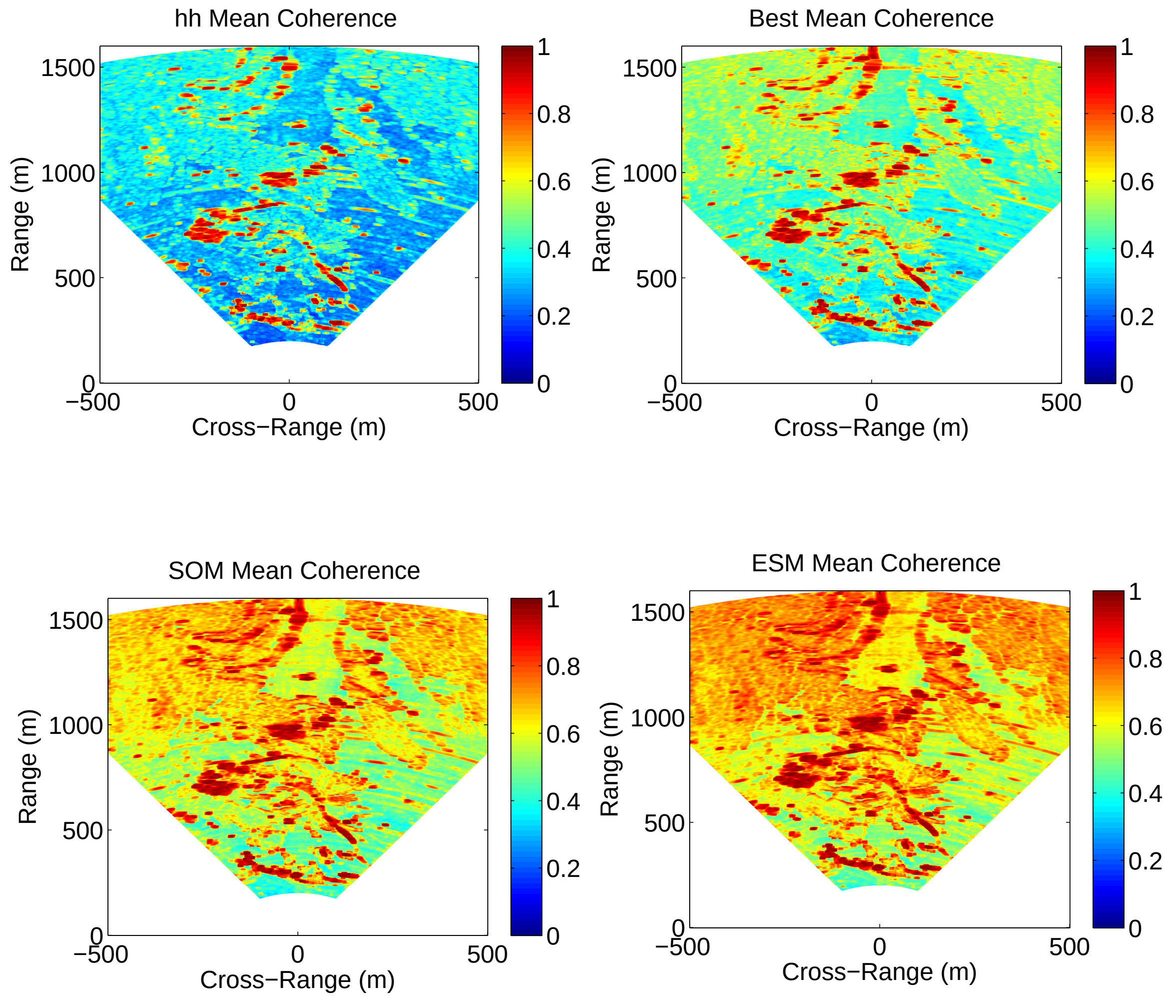

- *ESM* and *SOM* techniques are producing the greatest coherence improvement.
- The coherence improvement is higher in areas with low vegetation and bare surfaces compared with the few urban areas, which already presented high coherencies with *hh*
- The improvement in translated into a higher density of useful pixels

Coherence Optimization Techniques Comparison

Pixel candidates presenting a mean coherence above 0.7, which corresponds to a phase standard deviation of 5º
ML= 9x9

METHOD	NUMBER OF PIXELS
hh	17553 (2.4%)
hv	11638 (1.6%)
vv	18280 (2.5%)
Best	30345 (4.2%)
SOM	**45748 (6.4%)**
ESM	**53095 (7.4%)**

Threefold increase of the number of pixel candidates

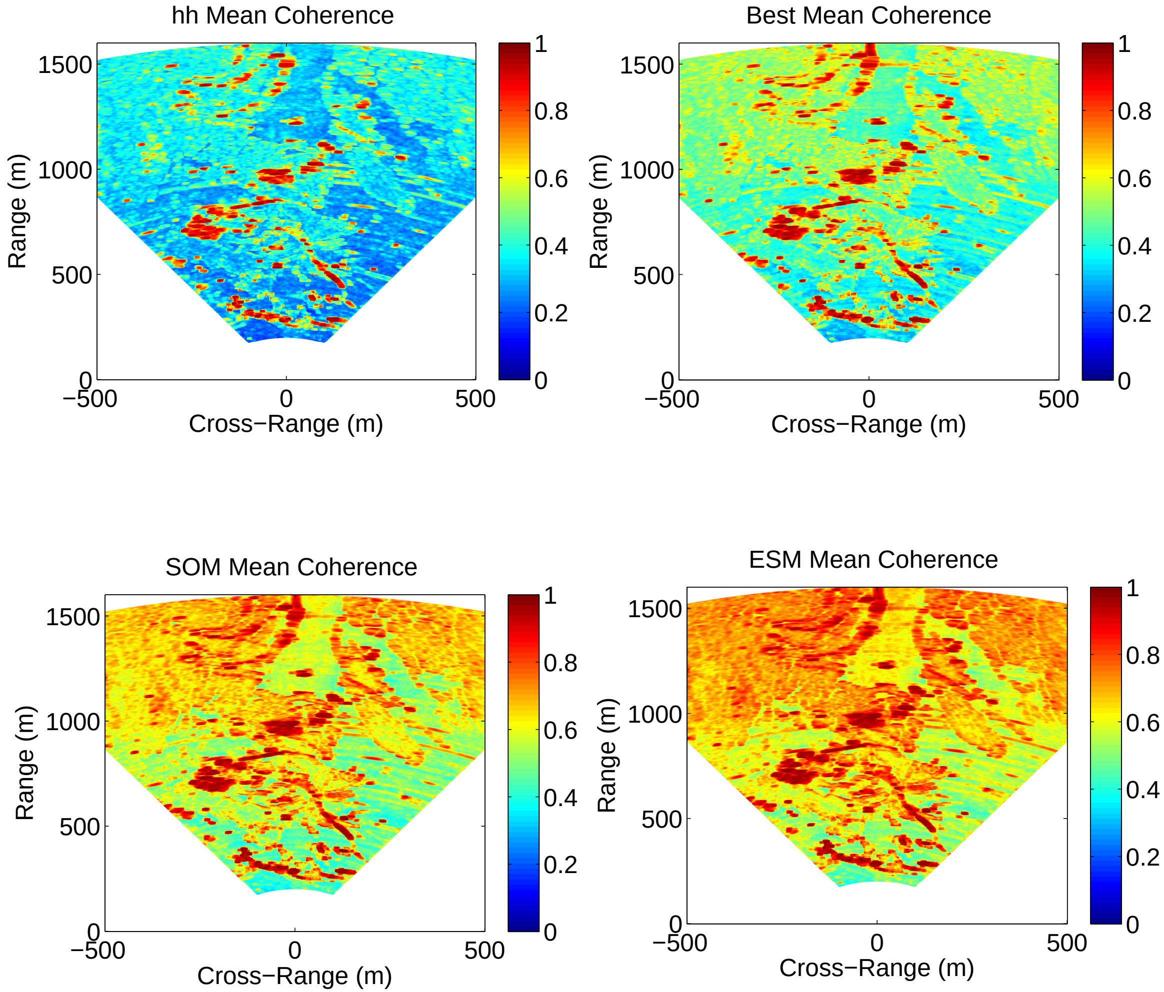

Coherence Optimization Techniques Comparison

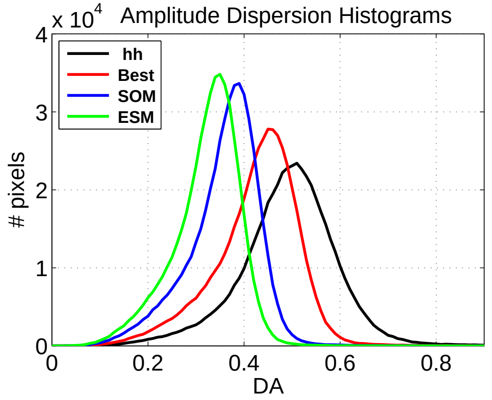

- *ESM* and *SOM* techniques are producing the greatest D_A improvement.
- The D_A improvement is higher in in areas with low vegetation than in the urban areas, which already presented low values of D_A with *hh*
- The improvement in translated into a higher density of useful pixels

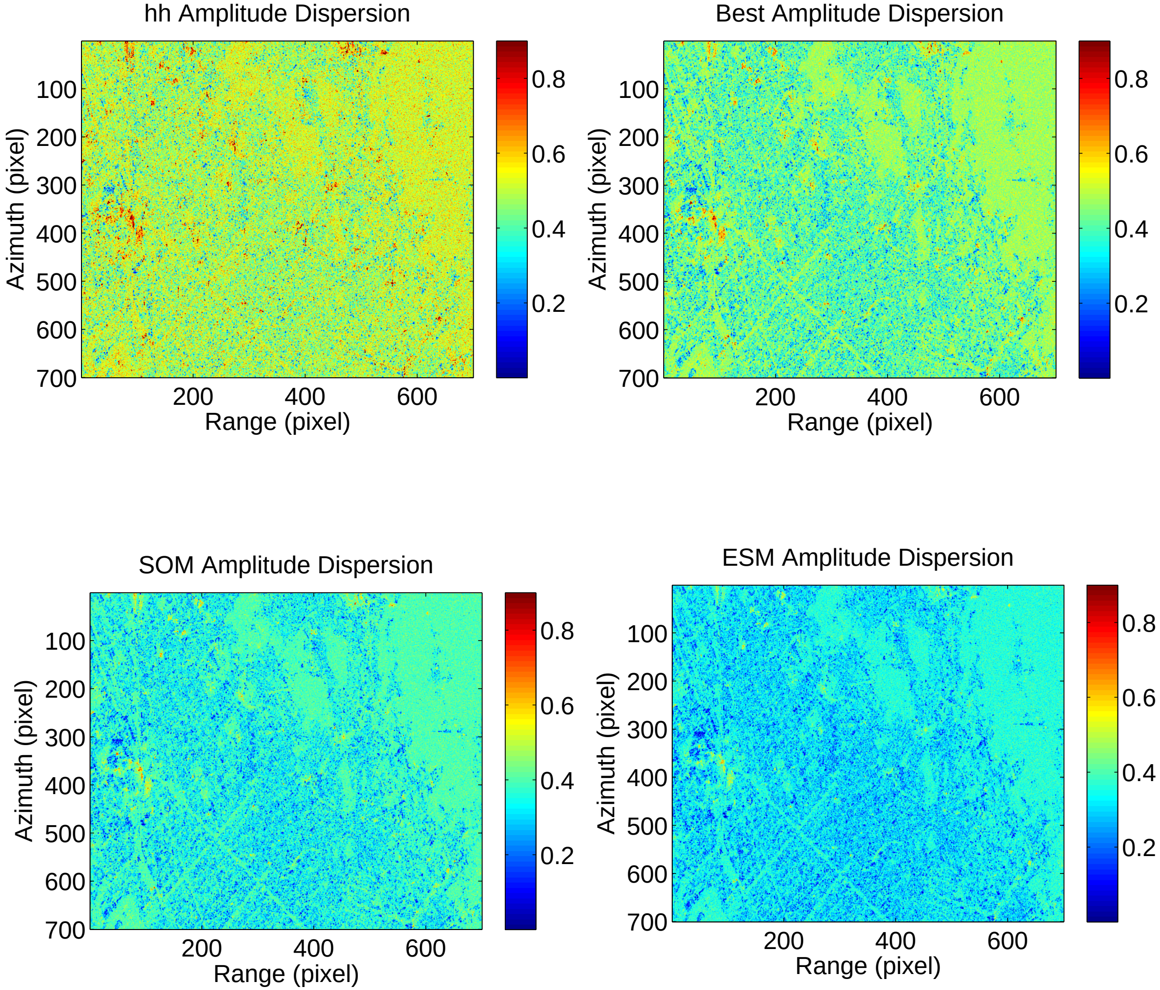

Coherence Optimization Techniques Comparison

Pixel candidates presenting DA value below 0.25, which corresponds to a phase standard deviation of 15º

METHOD	NUMBER OF PIXELS
hh	*9398 (1.9%)*
hv	*8522 (1.7%)*
vv	*9927 (2.0%)*
Best	*21721 (4.4%)*
SOM	***40032 (8.1%)***
ESM	***71702 (14.6%)***

Increase of a factor seven in the number of pixel candidates

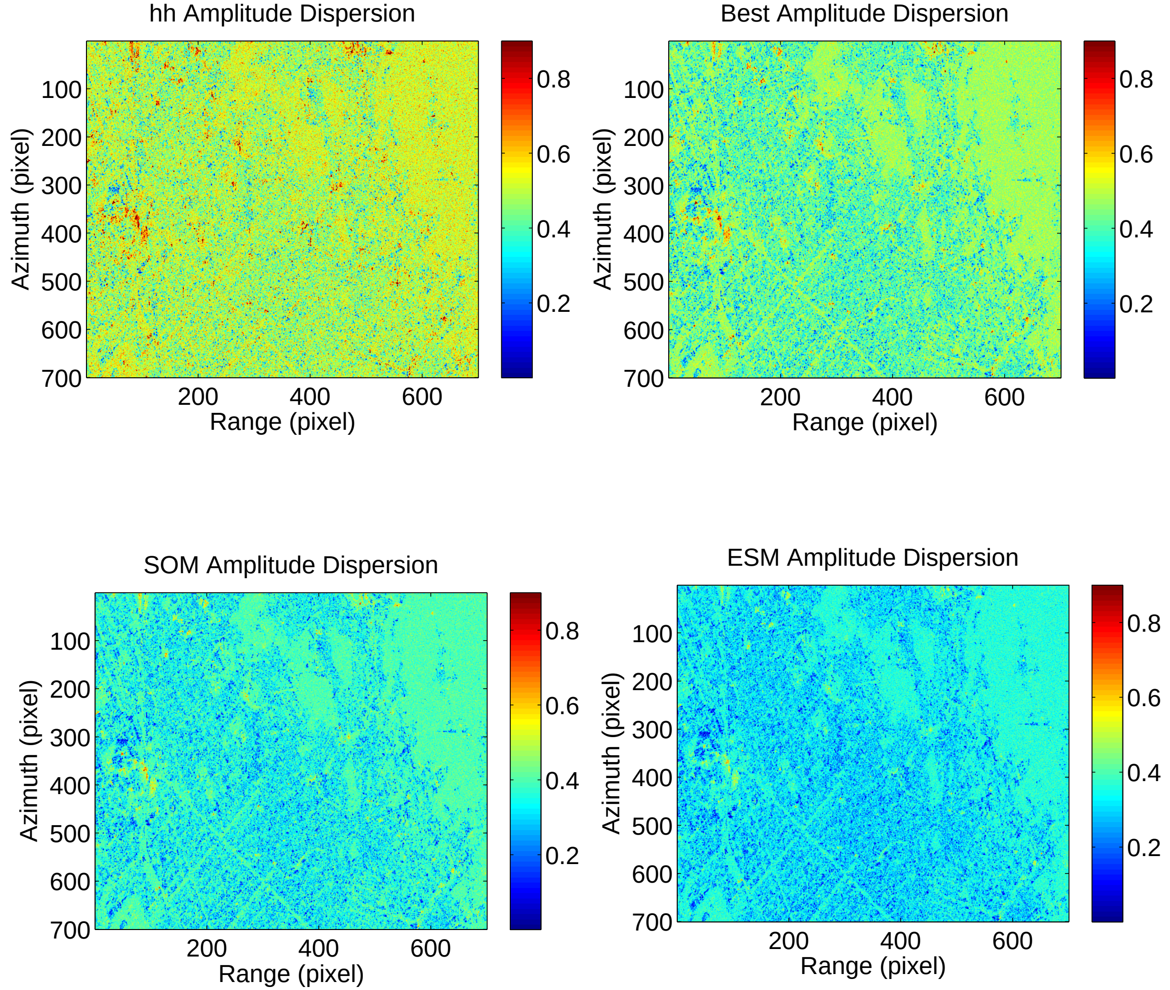

Polarimetric DInSAR processing

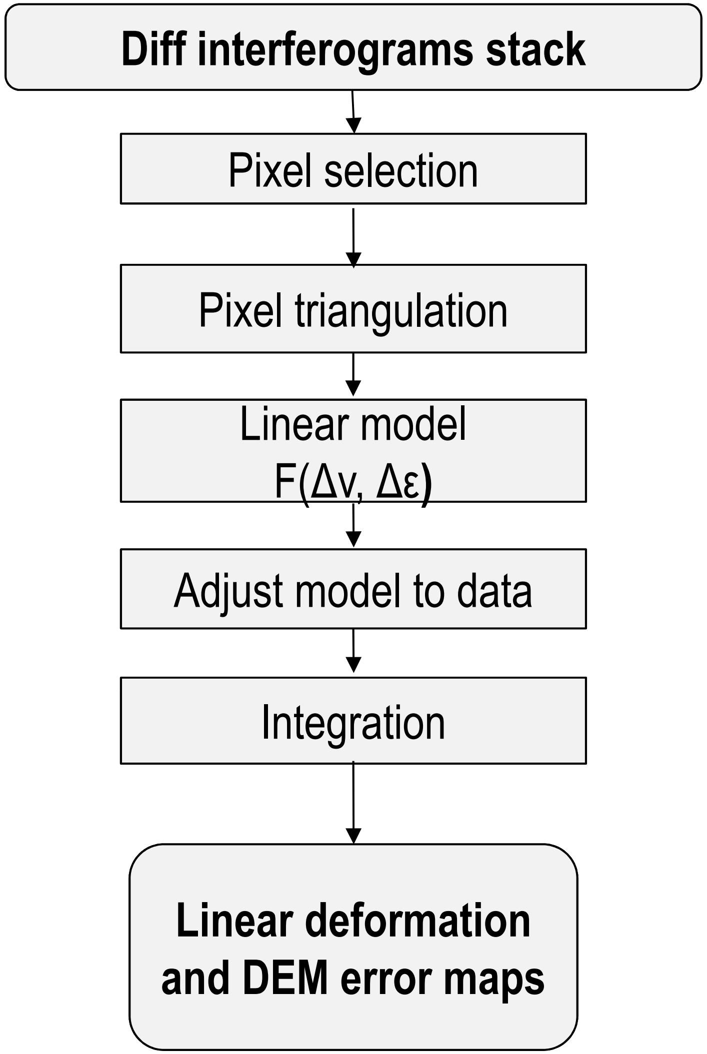

- **Differential Phase**: Information about terrain deformation between acquisitions.
- **Pixel Selection**: Along time coherence stability.
- **Triangulation**: Work with the relative phase between pixels to avoid unwrapping.
- **Phase Linear model**: Adjust phase increments to a linear model depending on Δv and Δε.

$$\Delta\phi(\Delta v, \Delta\varepsilon) = \frac{4\pi}{\lambda} T \Delta v + \frac{4\pi}{\lambda} \frac{B}{R \sin\alpha} \Delta\varepsilon$$

- **Integration**: Obtain deformation velocity and DEM error absolute values from the relative values.

Fully-Polarimetric DInSAR processing

Opt Diff interferograms stack

↓

Pixel selection

↓

Pixel triangulation

↓

Linear model
F(Δv, Δε)

↓

Adjust model to data

↓

Integration

↓

Linear deformation and DEM error maps

- **Differential Phase**: Information about terrain deformation between acquisitions.

- **Pixel Selection**: Along time coherence stability.

- **Triangulation**: Work with the relative phase between pixels to avoid unwrapping.

- **Phase Linear model**: Adjust phase increments to a linear model depending on Δv and Δε.

$$\Delta\phi(\Delta v, \Delta\varepsilon) = \frac{4\pi}{\lambda} T \Delta v + \frac{4\pi}{\lambda} \frac{B}{R \sin\alpha} \Delta\varepsilon + \Delta\phi_{POL}$$

- **Integration**: Obtain deformation velocity and DEM error absolute values from the relative values.

DInSAR results. Coherence optimization

- **SINGLE POL HH**

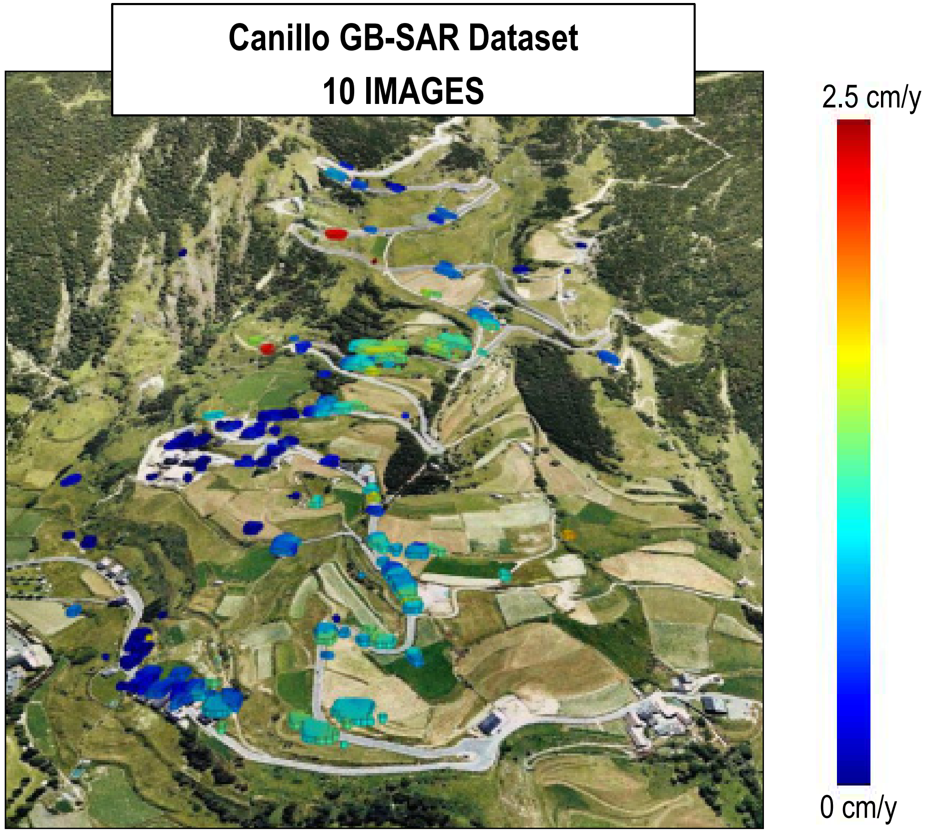

-10 X-band GB-SAR images

- Coherence > 0.7 $\left(\sigma_\phi < 5^{\mathrm{o}}\right)$

- Multilook of 9x9

- Residual movement of the order 1.5 of centimetres per year.
- Top-left extreme of the landslide a sector presents irregular activity (~2.5 cm/y) → Cal Ponet

DInSAR results. Coherence optimization

- **BEST**

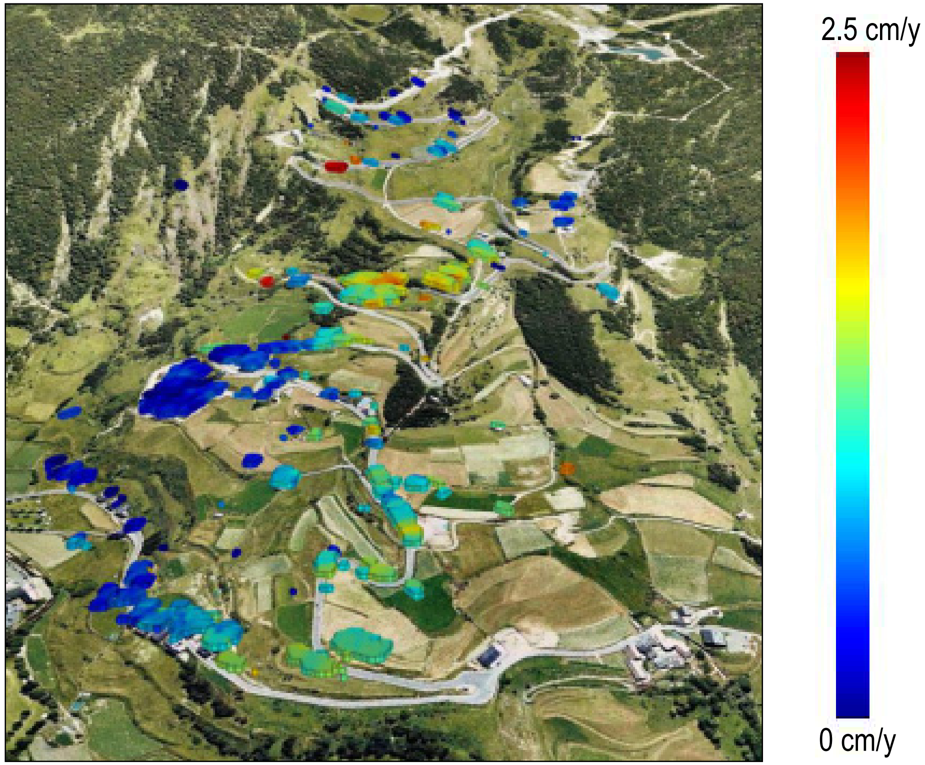

-10 X-band GB-SAR images

- Coherence > 0.7 $\left(\sigma_{\phi} < 5^{\circ}\right)$

- Multilook of 9x9

- Residual movement of the order 1.5 of centimetres per year.
- Top-left extreme of the landslide a sector presents irregular activity (~2.5 cm/y) → Cal Ponet

DInSAR results. Coherence optimization

- **SOM**

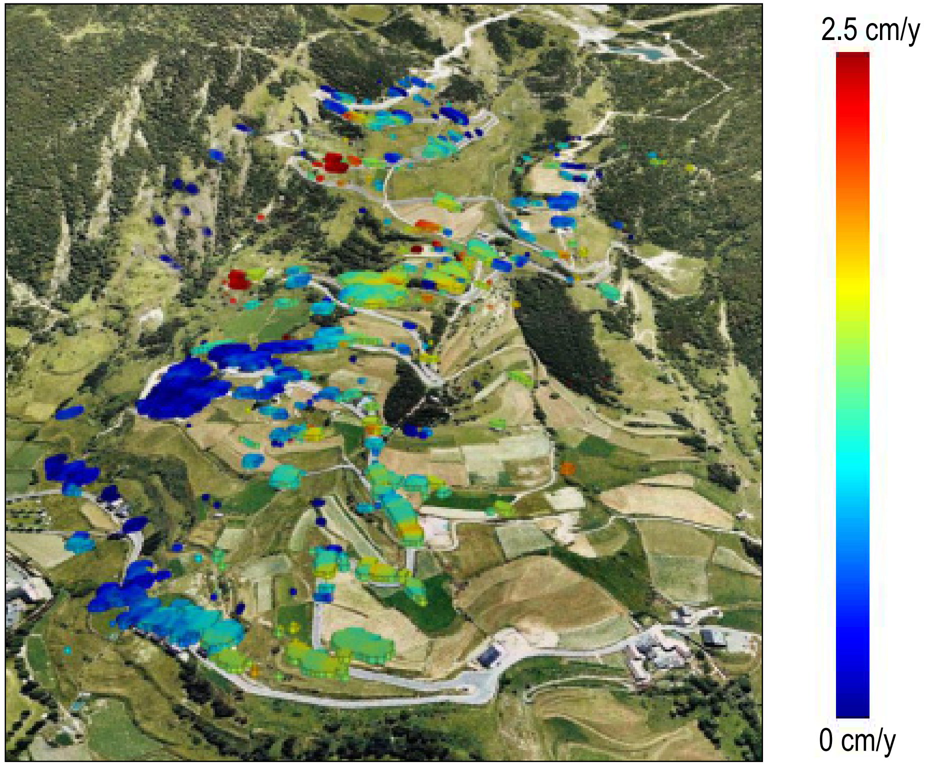

-10 X-band GB-SAR images

- Coherence > 0.7 $\left(\sigma_{\phi} < 5^{\circ}\right)$

- Multilook of 9x9

- Residual movement of the order 1.5 of centimetres per year.
- Top-left extreme of the landslide a sector presents irregular activity (~2.5 cm/y) → Cal Ponet

DInSAR results. Coherence optimization

- **ESM**

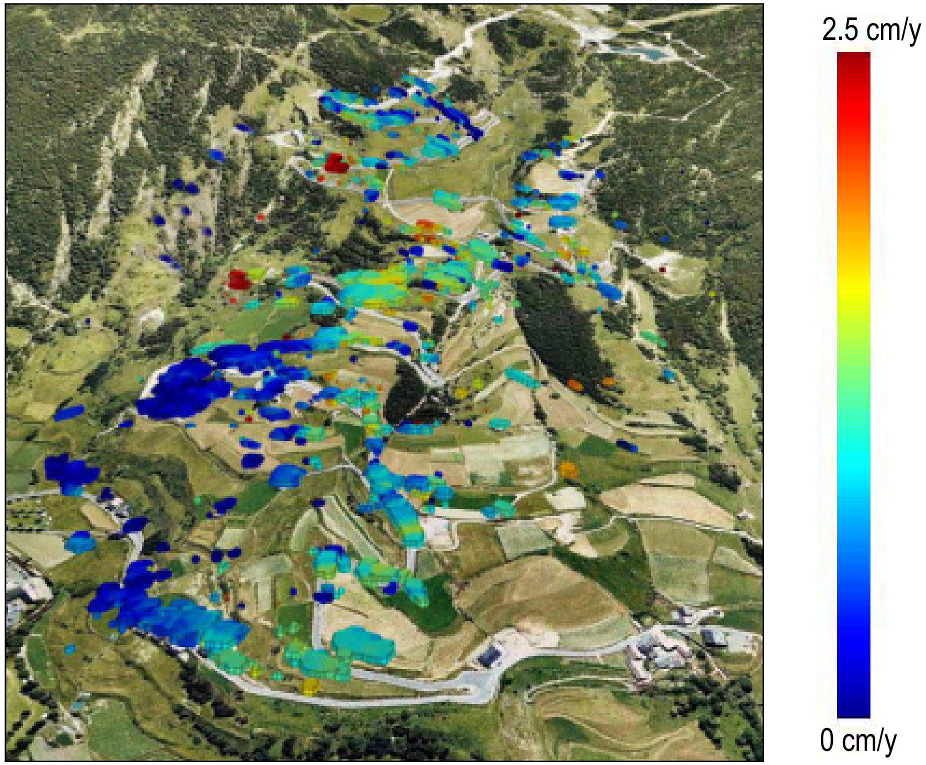

-10 X-band GB-SAR images

- Coherence > 0.7 $\left(\sigma_{\phi} < 5^{\circ}\right)$

- Multilook of 9x9

- Residual movement of the order 1.5 of centimetres per year.
- Top-left extreme of the landslide a sector presents irregular activity (~2.5 cm/y) → Cal Ponet

DInSAR results. D_A optimization

- **Best** $D_A > 0.25 \quad \left(\sigma_\phi < 15^o\right)$

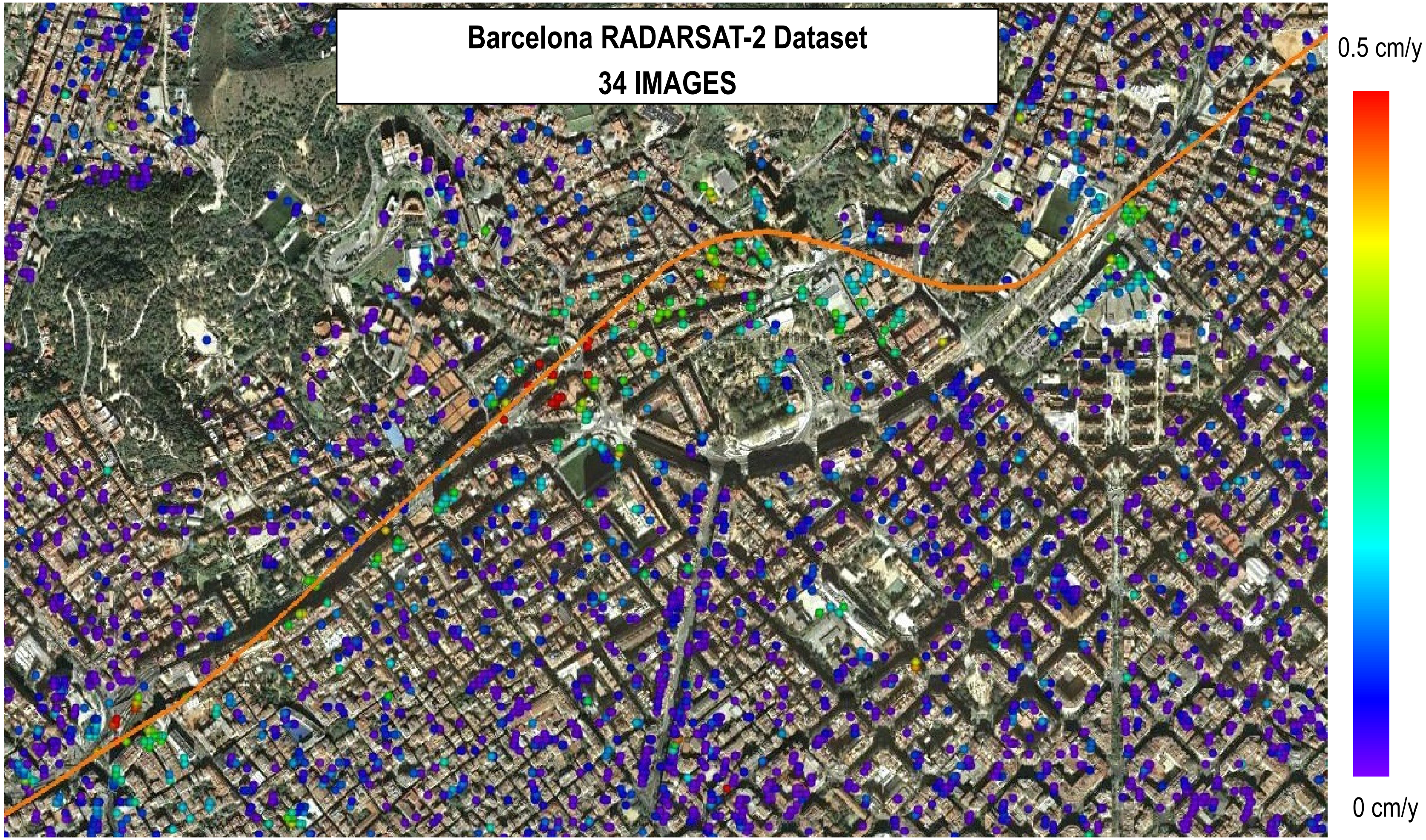

DInSAR results. D_A optimization

- **SOM** $D_A > 0.25$ $\left(\sigma_\phi < 15^{o}\right)$

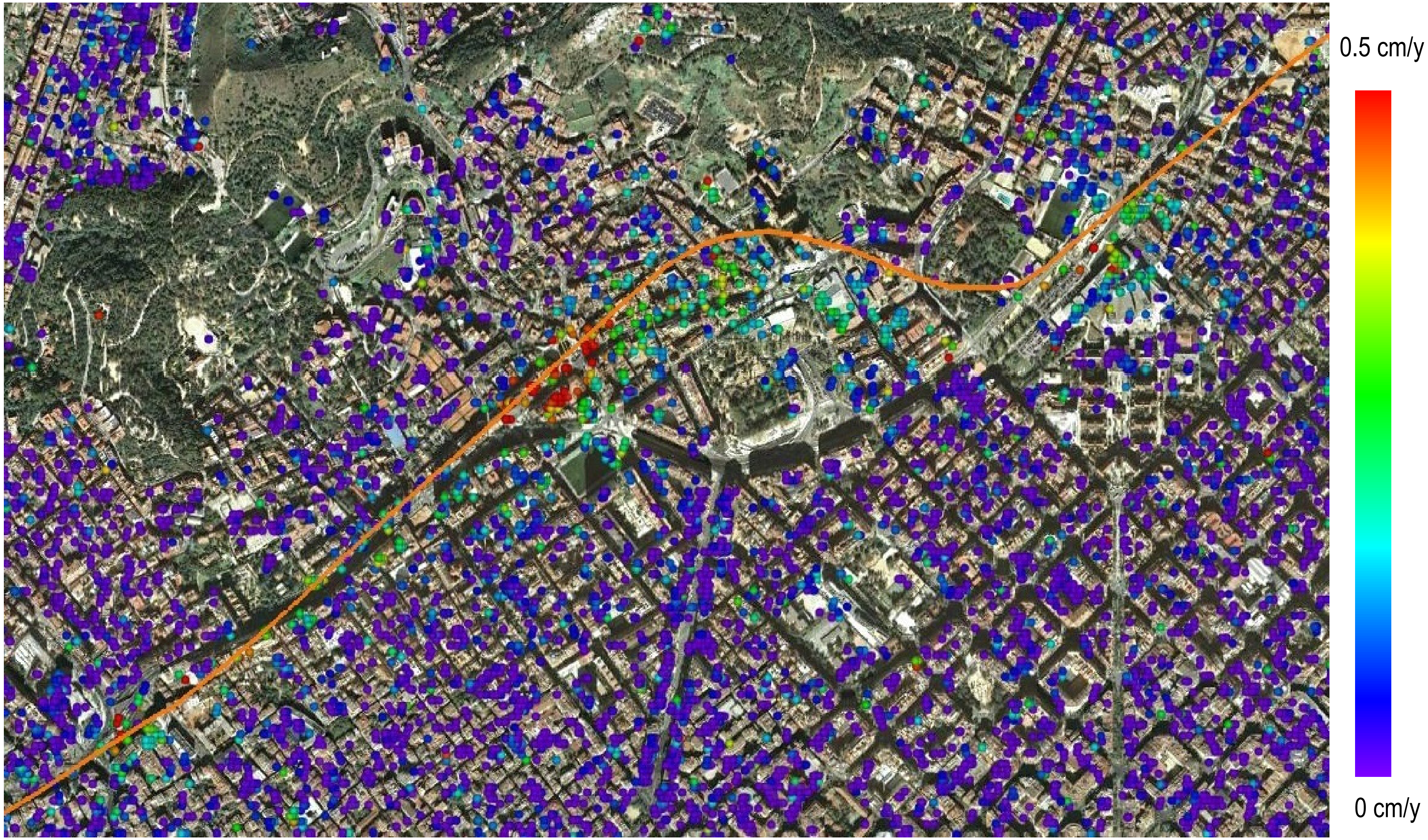

DInSAR results. D_A optimization

- **ESM** $D_A > 0.25 \qquad (\sigma_\phi < 15^{\circ})$

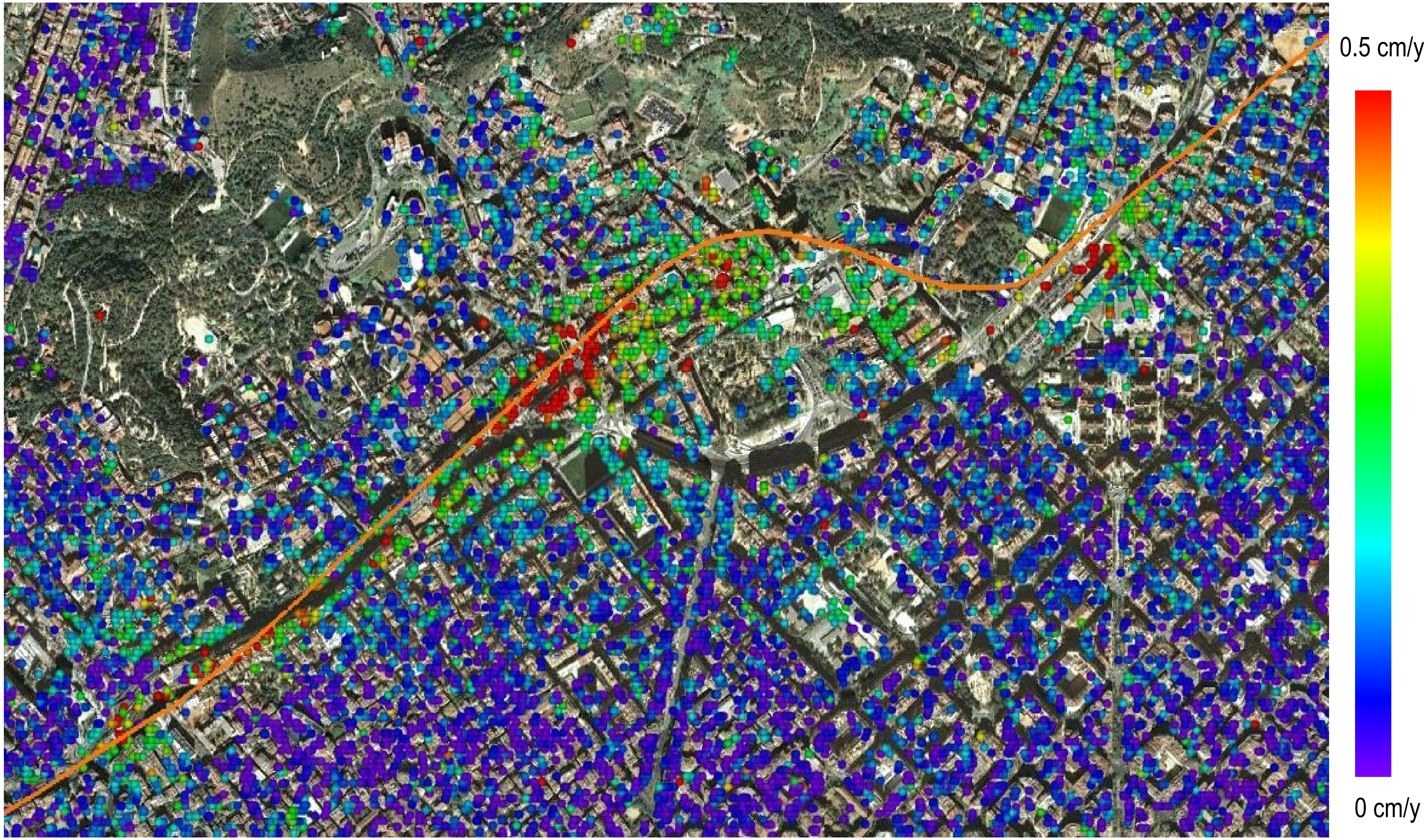

Conclusions

- In this work, general polarimetric optimization methods for its application in DInSAR processing have been presented
- *ESM* is able to get the best optimization values as it explores the full space of possible solutions, but with a high computational cost.
- *SOM* requires the optimization of a lower number of variables, which makes the optimization less costly, but the space of solutions is a subspace of *ESM*. As a consequence, *SOM* performance is usually below *ESM* in terms of phase improvement
- All this techniques can be extended to the D_A approach
- Once the optimized interferograms have been obtained, the DInSAR processing is straightforward as there are not practical differences with respect the single-polarization case
- DInSAR processing using polarimetric optimization techniques in the pixel selection process is compared with the classical single-polarimetric approach, achieving up to a threefold increase of the number of pixel candidates in the coherence case and up to a factor of seven in the amplitude dispersion case.

THANK YOU
FOR YOUR ATTENTION

QUESTIONS?

Acknowledgments

This research work received partial support from the Safeland project funded by the Commission of the European Communities (grant agreement 226479), from the Big Risk project (contract number BIA2008-06614) and the projects TEC2008-06764-C02-01 and TEC2011-28201-C02-01 funded by the Spanish MICINN. TerraSAR-X images have been provided by DLR in the framework of the scientific project GEO0878.